

Monte-Carlo approach to calculate the ionization of warm dense matter within particle-in-cell simulations

D. Wu,^{1,2} X. T. He,³ W. Yu,¹ and S. Fritzsche^{2,4}

¹*State Key Laboratory of High Field Laser Physics,
Shanghai Institute of Optics and Fine Mechanics, 201800 Shanghai, China*

²*Helmholtz Institut Jena, D-07743 Jena, Germany*

³*Key Laboratory of HEDP of the Ministry of Education,*

Center for Applied Physics and Technology, Peking University, 100871 Beijing, China

⁴*Theoretisch-Physikalisches Institut, Friedrich-Schiller-University Jena, D-07743 Jena, Germany*

(Dated: December 9, 2024)

A physical model based on Monte-Carlo approach is proposed to calculate the ionization dynamics of warm dense matters within particle-in-cell simulations, where impact ionization, electron-ion recombination and ionization potential depression (IPD) by surrounding plasmas are taken into consideration self-consistently. When compared with other models, which are applied in the literature for plasmas near thermal equilibrium, the temporal relaxation of ionizations can also be simulated by the proposed model with the final thermal equilibrium determined by the competition between impact ionization and its inverse process, i.e., electron-ion recombination. Our model is general and can be applied for both single elements and alloys with quite different compositions. The proposed model is implemented into a particle-in-cell (PIC) simulation code, and the average ionization degree of bulk aluminium varying with temperature is calculated, showing good agreement with the data provided by FLYCHK code.

PACS numbers: 52.38.Kd, 41.75.Jv, 52.35.Mw, 52.59.-f

I. INTRODUCTION

Warm dense matter (WDM) [1–3], with density 0.1 to 10 times that of solid and temperature 1 to 100 eV, is commonly found in astrophysics as well as in high-energy density physics experiments [4, 5]. Until the present, however, the properties of WDM are not well understood and are difficult to predict theoretically. This is because neither the models of condensed-matter nor from high-temperature plasmas are well suited for describing the intermediate regime of WDM.

Detailed information about the thermodynamic states, such as ionization distributions, is of importance in uncovering the involved physical mechanisms. The widely used models predicting an average ionization degree of atoms are Thomas-Fermi model [6] and Saha [7] ionization model, however both of the models assume that plasma conditions are near thermal equilibrium. For laser produced plasmas and intense beam solid interactions, where many of the involved physical mechanisms take place at the sub-pico-second or pico-second scales [8–11], the equilibrium assumption is no longer correct. To account for the temporal evolution of the plasma ionization, an impact model based on electron-ion collisional cross sections has been explored [12–14], which allows to calculate ionization values in much more natural manner. This model directly describes the inter-particle interactions in the plasmas and thus, accounts for the multi-particle nature of real plasmas. Although this impact ionization model allows improvements in dealing with non-equilibrium plasmas, it is still not complete since it does not account for the inverse process, such as electron-ion recombination [15–18]. Besides, the ionization poten-

tial depression (IPD) should be taken into account when dealing with high density plasmas [19–25], however it is also ignored in the considered model [12–14].

The main challenge to understanding the ionization of WDM is to incorporate self-consistently the non-linear behaviour in such strongly coupled dynamical systems, i.e., the matter’s response to the surrounding plasmas through impact ionization, recombination and IPD, and plasma’s response to the material through the dependence of plasma’s temperature and density on ionizations and recombinations.

To describe the ionization dynamics of WDM more systematically, we here propose and analyse a Monte-Carlo approach that can be configured and embedded into existing particle-in-cell (PIC) simulation codes. In this approach, we use a collection of macro-particles to describe a plasma of finite ion or matter density. Here, a macro-particle can be regarded as the ensemble of real particles, where a macro-particle can be regarded as a group of particles with “same” mass, charge state, position and momentum. The electrons are classified moreover into bound and free ones, where the former are regarded as part of ions or atoms, and the latter are isolated as part of surrounding plasmas. Since we consider a collection of large number of particles and the temporal evolution of the system takes place at pico-second scales, the fine structures, such as sub-shell configurations, excitations and their inverse processes, are ignored in the present model. Only the dominant physical processes are taken into account, i.e., impact ionization and recombinations. Furthermore, the IDP effects, which are determined by plasma density and temperature, should also be taken into account. This is because the depression of

ionization energy of ions or atoms by the IPD effects will then, in turn, affect both impact ionization and recombination processes.

The paper is organized as follows. The physical model concerning impact ionization, electron-ion recombination and IPD are introduced in Sec. II. In Sec. III, the model is embedded into PIC simulation code. The average ionization degree of bulk aluminium varying with temperature is calculated by the PIC code, which shows good agreement with the data provided by FLYCHK code. Furthermore, we also explore the ionization dynamics of alloys in this section. Summary and discussion are given in Sec. IV.

II. PHYSICAL MODEL

When temperature of plasma is high with the kinetic energy of free electrons exceeding the ionization potential of ions or atoms, there exists a possibility that the ion or atom will lose a bound electron by the colliding with energetic free electrons, and we call this process as impact ionization. Simultaneously, for cold and dense plasmas, free electrons and charged ions tend to recombine together, and we call this process as electron-ion recombination. Different from isolated atom or ion, the Debye screening of free electrons would dramatically influence the atomic structure of ions that embedded in dense plasmas, resulting in the lowering of the ionization potential. The above three processes are usually ignored in high temperature and low density plasmas, such as laser wake field acceleration. While for dense plasma and warm dense matter regime, they are so important that become the dominant processes of the considered system. In this section, an impact ionization model based on electron-ion collisional cross sections, an electron-ion recombination model based on three-body-recombination and the IPD effects based on Stewart's theory are explored and implemented in PIC simulations.

a. Impact ionization By establishing an electron-ion or atom collisional pair and taking into account the energy of the incoming electron as well as the ionization state of the ion, a cross section of ionization can be derived. The pioneering work was done by Lotz [26], with the formula of the total cross section as follows

$$\sigma^{\text{ci}} = \sum_{i=1}^N a_i q_i \frac{\ln(E/P_i)}{EP_i} [1 - b_i \exp(-c_i(E/P_i - 1))], \quad (1)$$

where E is the energy of impact electron, P_i is the binding energy of electron in the i -th sub-shell, q_i is the number of equivalent electron in the i -th subshell, and a_i , of unit $10^{-14} \text{cm}^2 \text{eV}^2$, b_i and c_i are individual constants which are determined by experiment measurements or theoretical predictions. Ref. [26] also tabulates these ionization cross sections, and this table is applied in our computations below. Following the work of Lotz, the ionization cross section among neighbouring levels, such as, Al-II to

Al-III, can be formulated as follows,

$$\sigma_i^{\text{ci}} = a_i q_i \frac{\ln(E/P_i)}{EP_i} [1 - b_i \exp(-c_i(E/P_i - 1))], \quad (2)$$

with $E \geq P_i$, where P_i is the ionization potential. Let us note, however, the fine structure levels are ignored in Lotz's model, for which the ionization stage is treated as from the ground state to the next ground state. Furthermore, the electron impact ionization cross section can also be calculated using the relativistic multi-configuration Flexible Atomic Code (FAC) [28], where multitude of ionization cross sections can be generated by the FAC between the fine structure levels of the initial and final states, and finally combined into a single effective cross section as obtained from a summation over the initial and average over the final states. The impact ionization rate of ion or atom is

$$\nu_i^{\text{ci}} = \int_{P_i}^{\infty} v_e \sigma_i^{\text{ci}}(E) f_e(E) dE, \quad (3)$$

where E , v_e , and f_e are energy, velocity and density of impact electrons with energy between E and $E + dE$. In PIC simulations, the integral stands for summarizing over all electrons that reside within the same cell as the given ion of interest. The expression for ν_i in this form can be time-consuming as it requires a double loop over all ions and electrons in the cell. Following the idea presented in Ref. [13] and taking advantage of the specific scaling of the ionization cross section and electron velocity with energy, i.e., $\ln(E)/E$ and \sqrt{E} , respectively, their product is not sensitive to E and can be taken outside the integration. When replaced by their averaged values, the impact ionization rate takes the form

$$\nu_i^{\text{ci}} = \sigma_i^{\text{ci}}(\bar{E}) \bar{v} n_e (\text{s}^{-1}). \quad (4)$$

A loop over the electrons updates the average electron energy \bar{E} , velocity \bar{v} and electron density n_e , of unit cm^{-3} , in each computational cell once per time step. Then Eq. (4) is applied for each ion keeping track of which cell it belongs to. The ionization probability of the ion of interest is $p_i^{\text{ci}} = 1 - \exp(-\nu_i^{\text{ci}} \delta t)$, where δt is the simulation time step. We increase the ionization degree by one unit for each ion and simultaneously put in an electron with the same position, velocity and weight as its host ion randomly when condition $r > p_i^{\text{ci}}$ is satisfied, where r is the computer generated random number. To ensure that the energy remains conserved in the computations, we reduce local kinetic energy by distributing a momentum reduction to all local electrons, which is equivalent to the ionization energy.

b. Electron-ion recombination The ionization balance of a plasma is determined by the competing processes of impact ionization and recombination, as well as various excitation/de-excitation processes. In particular, the recombination of electrons and ions takes place mainly by three different reaction modes, the dielectronic (DR), radiative (RR) and three-body recombinations (TBR), respectively [15]. As we have analysed,

in our model only ground state of ions and atoms are concerned, the contributions of DR are averaged out. Note that, RR is the inverse of the direct photo-ionization, while TBR is the inverse process of electron impact ionization. The RR process is known to predominantly fill the low-lying Redberg states, while TBR is mainly responsible in rapidly bringing the high Rydberg states into equilibrium [15]. Thus, the contributions of recombinations mainly come from the TBR process, with $e + e' + A^Z \rightarrow A^{ZM} + e''$, where $ZM = Z - 1$ with Z of the ion charge state. In the TBR, the excess energy released by the recombining electron is carried away by the outgoing electron e'' , so that the TBR does not involve any emission of photons. A simple expression for TBR rate, which is usually obtained from the relying impact ionization formula by detailed balance, is as follows [15],

$$\nu_i^{rc} = 8.222 \times 10^{-28} \times n_e n_i Z^3 / T_e^{4.5} (\text{eV}) (\text{s}^{-1}). \quad (5)$$

All the TBR formulas exhibit this behaviour [16–18], except for the slightly different numerical factors. In PIC simulations, the electron temperature T_e , and electron density n_e can be generated by a loop over the electrons in each computational cell once per time step. Then Eq. (5) is applied for each ion after calculating the ion density n_i in the same cell. The recombination probability is $p_i^{ir} = 1 - \exp(-\nu_i^{ir} \delta t)$, where δt is the simulation time step. We decrease ionization degree by one unit for each ion randomly whenever the random number r satisfies $r > p_i^{ir}$. Again to ensure that the energy remains conserved, the local kinetic energy, equivalent to the ionization energy, is increased, through a similar way as we have done in impact ionizations, by distributing a momentum modification to all local electrons. To ensure the conservation of remain particles, the local plasma density, equivalent to the ionization recombination, is reduced by distributing a weight modification to all local free electrons.

c. IPD by surrounding plasmas The calculation of both impact ionization and electron-ion recombination requires values of ionization potentials, which, in principle, can be generated or obtained from data bases of National Institute of Standard and Technology (NIST). The ionization potential of aluminium atom (Al I) and ions are listed in Table I, which are calculated based on the isolated atom or ion model. However in a plasma of finite density and temperature, the ionization potential of a given ion is influenced not only by its own bound electrons but also by the surrounding free electrons, which, in turn, will affect both impact ionization and recombination processes. Therefore, the phenomenon of ionization-potential depression for ions embedded in the plasma are of crucial importance for modelling atomic processes within dense plasmas. We refer to the theory of IPD introduced by Stewart [20], which yields ion-sphere and Debye-Huckel potential models as approximate limiting cases and could provide results over essentially the entire range of temperature and densities of plasmas for which appreciable ionization exists. Let us here consider an

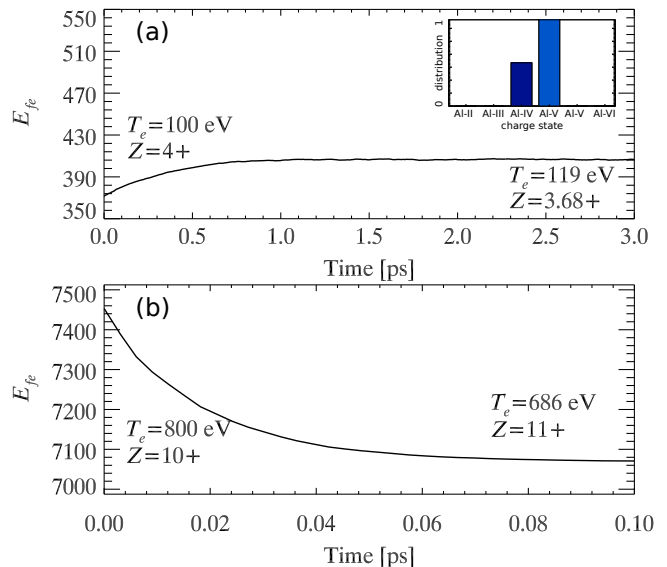


FIG. 1. (color online) (a) The total plasma energy, by summarizing over all free electrons within a computational cell, as a function of time, where the initial plasma temperature is 100 eV and pre-defined $Z = 4$ charge state. (b) The same as shown in (a), but with initial temperature 800 eV and pre-defined charge state of $Z = 10$. The inset over (a) is the final ionization distributions of aluminium after 3 ps relaxation.

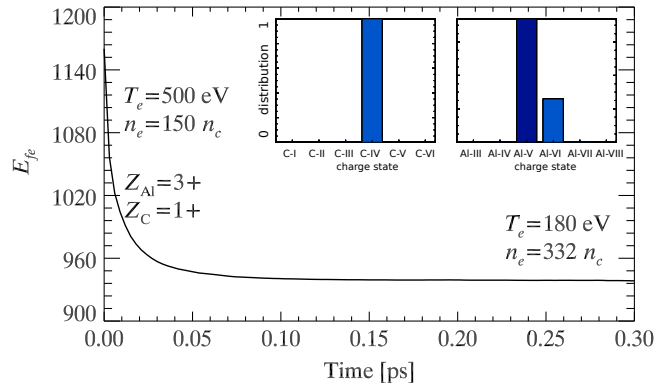


FIG. 2. (color online) The total plasma energy (or free electron energy) within a computational cell as a function of time, where the initial temperature of aluminium carbide is 500 eV with pre-defined charge states of $Z_{Al} = 3$ and $Z_C = 1$ and plasma density of $150n_c$. The inset is the final ionization distributions of aluminium and carbon after 0.3 ps relaxation.

atom or ion, i , fixed in a sea of free electrons and ions at kinetic temperature T_e . The free electrons are described by relativistic Fermi-Dirac statistics and the ions by non-relativistic Maxwell-Boltzmann statistics. For such a distribution of plasma electrons, the average electro-static potential near i can be evaluated by Poisson equations. It is this potential that cause the IPD effects of surrounding plasmas. The contribution of bound electrons to IPD are excluded, since they are already present in the isolated ions.

TABLE I. Ionization potential of aluminium atom and ions from NIST [27] as implemented in our model. See text for explanations.

Al	1	2	3	4	5	6	7	8	9	10	11	12	13
eV	5.980	18.80	28.40	119.9	153.8	190.4	241.4	284.5	330.1	398.5	441.9	2085.	2300.

Following Stewart's theory [20], the lowering of ionization potential is described by the expressions,

$$\Delta P = \{[3(Z+1)K+1]^{2/3} - 1\}T_e/2(Z+1), \quad (6)$$

where T_e is temperature of free electrons, $K = Ze^2/\lambda_d T_e$ with $\lambda_d = \sqrt{T_e/4\pi Z n_e}$ representing the Debye length of free electrons. For large K , according to Eq. (6), ΔP is reduced to Ze^2/λ_d which is the limit of Debye-Huckel model. When K is small, ΔP equals to $3Ze^2/2a$, which is the limit of ion-sphere model, with $a = \sqrt[3]{3Z/4\pi n_e}$ representing the radius of ion-sphere. For high density plasmas, the IDP would have a significant effect on lowering of ionization potential. For example, ΔP of Al VII (with the isolated ionization potential 240 eV) can be as large as 100 eV for bulk aluminium (2.7 g/cm^3) with temperature T_e below 300 eV. Apart from such a semi-empirical treatment of ionization potential depressions, the IDP effects can also be described from multi-body-quantum-mechanical methods [22, 23]. We compared the estimation from Stewart's formula with that from references [22, 23], and found the calculation methods exhibit similar behaviour, though with slightly different numerical values. In PIC simulations, the electron temperature T_e and density n_e can be generated by a loop over the electrons in each computational cell, attached to which the Debye length λ_d is evaluated. Using Eq. (6) and the isolated ionization potential value from NIST data bases, the modified ionization potential, i.e., $P - \Delta P$, is updated for each ion at every computational cell per time step.

III. APPLICATIONS

The physical model is embedded in a recently extended version of PIC code based on LAPINE [29], with which the tunnelling ionization have already been implemented in by one of us [30]. In PIC simulations, we only need to consider a few computational cells, connected by periodic boundaries conditions, with each cell contains 800 ion macro-particles and 800 electron macro-particles initially. In this section, we present several case studies of the ionization dynamics of bulk aluminium (single) and aluminium carbide (alloy). The density of bulk aluminium in our case studies is 2.7 g/cm^3 , thus, the aluminium ion density is $60n_c$, with $n_c = 1.1 \times 10^{21}/\text{cm}^3$. Fig. 1 shows the temporal evolution of the plasma energy, summarizing over all free electrons within one computational cell (energy density of plasmas), where the initial aluminium temperature is 100 eV [Fig. 1 (a)] and 800 eV [Fig. 1 (b)] with pre-defined charge states of $Z = 4$ [Fig.

1 (a)] and $Z = 10$ [Fig. 1 (b)]. From Fig. 1 (a), we can see that the energy density of plasmas increases with time, after about 3 ps temporal relaxation, equilibrium is reached, with the final temperature of $T_e = 119 \text{ eV}$ and average charge degree of $Z = 3.68$. Following the temporal relaxation as shown in Fig. 1 (a), the electron-ion recombination rate of aluminium at the very beginning is larger than impact ionization rate, and, therefore, the recombination processes lead to the increase of plasma energy and reduction of average ionization degree, until the arrival of equilibrium. Fig. 1 (b) indicates that at initial time, the impact ionization rate of aluminium is larger than electron-ion recombination. Similarly, the impact ionization would reduce the plasma energy and increase the average ionization degree.

Our model is general and can be applied for both single elements and alloys with quite different compositions. The aluminium carbide, chemical formula Al_4C_3 , is a carbide of aluminium with density 2.36 g/cm^3 . Fig. 2 shows the temporal evolution of energy density of plasmas, where the initial aluminium carbide temperature is 500 eV with pre-defined charge states of $Z_{\text{Al}} = 3$ and $Z_{\text{C}} = 1$ and plasma density of $150n_c$. As seen from this figure, the equilibrium is reached after 0.3 ps of temporal relaxation with a plasma temperature of $180n_c$ and free electron density of $332n_c$. The inlet is the final ionization distributions of aluminium and carbon.

In our model, different strategies were used to ensure that the total number of particles remain conserved. The reduction of electrons due to recombination is through distributing a weight modification to all local free electrons, which does not change the number of macro-particles. While the increase of electron due to impact ionization is through placing *new* macro-particles to the cell of interest. The major computational effort in the simulation arises from the number of macro-particles. To solve this problem, a particle-merging technique is configured and applied. Considering two electrons with position \mathbf{r}_a and \mathbf{r}_b , momentum \mathbf{p}_a and \mathbf{p}_b , gamma factor γ_a and γ_b , as well as weight w_a and w_b , we have the merging weight as $w = w_a + w_b$, merging position as $\mathbf{r} = (w_a\mathbf{r}_a + w_b\mathbf{r}_b)/w$, merging gamma factor as $\gamma = (w_a\gamma_a + w_b\gamma_b)/w$, and the merging momentum as $\mathbf{p} = (w_a\mathbf{p}_a + w_b\mathbf{p}_b)/w$. In practice, the equation, $\gamma = \sqrt{p^2 + 1}$, is not always satisfied for the *merged* particles. To solve this problem, a coefficient of $\eta = \sqrt{(\gamma^2 - 1)/p^2}$ is multiplied to replace the old merging momentum, with $\mathbf{p} = \eta\mathbf{p}$.

The case shown in Fig. 1 (a) is re-run by including the merging-particle technique. Fig. 3 (a) shows how the energy density of plasmas evolves in time, while Fig. 3

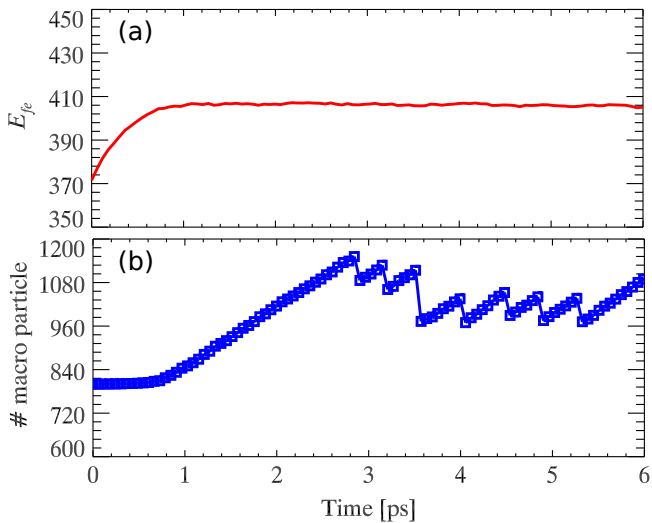


FIG. 3. (color online) (a) The total plasma energy within one computational cell as a function of simulation time, where the initial aluminium temperature is 100 eV with pre-defined $Z = 4$ charge state. (b) the corresponding temporal fluctuation of the number of macro-particles in PIC simulations.

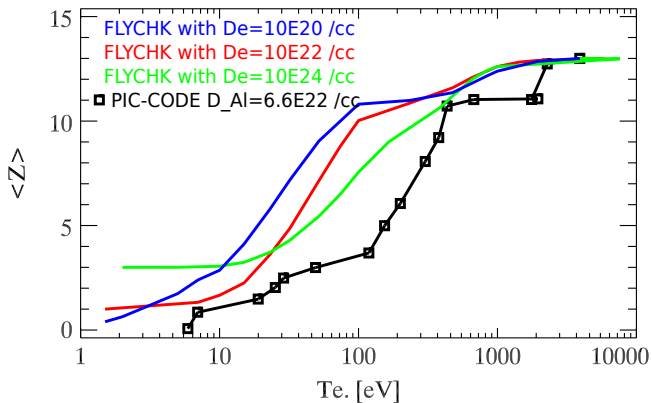


FIG. 4. (color online) The average ionization degree of bulk aluminium as a function of plasma temperature. Black square is picked up from the equilibrium states calculated by our PIC simulations. Blue, red and green lines are the corresponding average ionization degrees with fixed plasma density of 10^{20} cm^{-3} , 10^{22} cm^{-3} and 10^{24} cm^{-3} calculated by FLYCHK code.

(b) displays the corresponding number of macro particles. Both the energy evolution and final equilibrium shown in Fig. 3 (a) is exactly the same as shown in Fig. 1 (a). In the simulation, the merging takes place at pre-defined times. As we can see, the dropping of the total number of macro particles does not affect the energy evolution or final equilibrium. By using this technique, the simulation burden can be dramatically released.

Following the routine described above, we plot the variation of average ionization degree of bulk aluminium with temperature. A collection of data picked from equilibrium represented by black squares is shown in Fig. 4. It

is indicated that with the increase of plasma temperature, the average ionization degree also increases accordingly. We also compare our results with that from FLYCHK [31, 32] code, in which the ionization calculation is also based on Saha ionization model [7]. In Fig. 4, blue, red and green lines are the corresponding average ionization degrees, calculated from FLYCHK code, as functions of temperature with fixed plasma densities of 10^{20} cm^{-3} , 10^{22} cm^{-3} and 10^{24} cm^{-3} . Note that in our calculations, the aluminium density is fixed, with $n_{Al} = 60n_c$, but let both the “plasma” (free electrons) density and ionization charge states free to change with time and temperature. Furthermore, the free electron density and average ionization degree of aluminium are connected by the relationship, $Z = n_e/n_{Al}$. Our calculation method reflects the ionization dynamics of materials in a more natural way, which is quite different from the model used in FLYCHK, where the average ionization degree is calculated with fixed free electron density. Although the calculation configuration is quite different, as we can see, the calculation results on variation of average ionization degree with plasma temperature are in good agreement.

However we still notice some slight difference between our calculation and that from FLYCHK code. At low temperature limit, i.e., temperature below 10 eV, the average ionization degree from our simulation is close to zero, while that calculated from FLYCHK depends on the plasma density. For plasma of density 10^{24} cm^{-3} , the average ionization degree is “3+”, while for plasma of density 10^{20} cm^{-3} , it is also close to zero. According to the calculations of FLYCHK code, both the calculation results, “3+” and “0”, make sense. For aluminium of density 2.7 g/cm^3 , i.e., $n_{Al} = 6.7 \times 10^{22} \text{ cm}^{-3}$, average charge degree “3+” means the plasma density is $2.0 \times 10^{23} \text{ cm}^{-3}$. The average charge degree “0.01+” corresponds to the plasma of density 10^{20} cm^{-3} . It is hard for us to judge the average ionization degree of a bulk aluminium at low temperature limit, if we follow the calculations of FLYCHK. For electron temperature between 400 eV and 2000 eV, it is indicated from our calculation that there exists an “ionization shelf”, meaning Al^{11+} is a very stable charge state. Following the ionization potentials of aluminium listed in Table. I, we can see that the ionization potential abruptly increases from $P_{11} = 441 \text{ eV}$ to $P_{12} = 2085 \text{ eV}$. The large ionization potential gap is due to the “solid” $1s^2$ core. Considering the stability of this “solid” core, the existence of “ionization shelf” seems reasonable.

IV. CONCLUSIONS AND DISCUSSIONS

In summary, a physical model based on Monte-Carlo approach is proposed to investigate the ionization dynamics of warm dense matter in PIC simulations. In our model, both impact ionization and electron-ion recombination are taken into account. Furthermore, the IPD affected by surrounding plasmas are also self-consistently

taken into consideration. When compared with other existing models which do not often include the relevant physical mechanisms at the sub-pico second or pico-second scales, our proposed model drops the constrain of thermal equilibrium conditions. Therefore, our model can be applied also for non-equilibrium processes.

The key issue related to impact ionization is the related cross section calculation, which can be calculated or generated either from Lotz's formula or from external simulation code, such as multi-configuration Flexible Atomic Code. The electron-ion recombination model is based on three-body-recombination. The IPD effect by surrounding plasmas is calculated by the model proposed by Stewart. Furthermore, the IDP effect can also be calculated by multi-body-quantum-mechanical methods. Both the calculation methods exhibit similar behaviour, except for the slightly different numerical values.

The proposed model is implemented into an existing particle-in-cell simulation code. The temporal relaxation of bulk aluminium and aluminium carbide is calculated. In order to release the calculation burden and simultaneously ensure the calculation accuracy, a merging particle technique is configured and applied. The variation of average ionization degree of bulk aluminium with temperature calculated from our model is compared with that from FLYCHK code, showing good consistency.

ACKNOWLEDGMENTS

D. Wu wishes to acknowledge the financial support from German Academic Exchange Service (DAAD) and China Scholarship Council (CSC), also thanks B. Goswami, J. W. Wang and S. Z. Wu at Helmholtz Institut-Jena for fruitful discussions.

-
- [1] T. G. White, N. J. Hartley, B. Borm, B. J. B. Crowley, J. W. O. Harris, D. C. Hochhaus, T. Kaempfer, K. Li, P. Neumayer, L. K. Pattison, F. Pfeifer, S. Richardson, A. P. L. Robinson, I. Uschmann, and G. Gregori, *Phys. Rev. Lett.* 112, 145005 (2014).
- [2] A. Pelka, G. Gregori, D. O. Gericke, J. Vorberger, S. H. Glenzer, M. M. Gunther, K. Harres, R. Heathcote, A. L. Kritcher, N. L. Kugland, B. Li, M. Makita, J. Mithen, D. Neely, C. Niemann, A. Otten, D. Riley, G. Schauermann, M. Schollmeier, An. Tauschwitz, and M. Roth, *Phys. Rev. Lett.* 105, 265701 (2010).
- [3] G. M. Dyer, A. C. Bernstein, B. I. Cho, J. Osterholz, W. Grigsby, A. Dalton, R. Shepherd, Y. Ping, H. Chen, K. Widmann, and T. Ditmire, *Phys. Rev. Lett.* 101, 015002 (2008).
- [4] M. Roth, T. E. Cowan, M. H. Key, S. P. Hatchett, C. Brown, W. Fountain, J. Johnson, D. M. Pennington, R. A. Snavely, S. C. Wilks, K. Yasuike, H. Ruhl, F. Pegoraro, S. V. Bulanov, E. M. Campbell, M. D. Perry, and H. Powell, *Phys. Rev. Lett.* 86, 436 (2001).
- [5] J. C. Fernandez, B. J. Albright, F. N. Beg, M. E. Foord, B. M. Hegelich, J. J. Honrubia, M. Roth, R. B. Stephens, and L. Yin, *Nucl. Fusion* 54, 054006 (2014).
- [6] D. Salzmann, *Atomic Physics in Hot Plasmas* (Oxford University Press, Oxford, 1998), pp. 2728.
- [7] I. H. Hutchinson, *Principles of Plasma Diagnostics* (Cambridge University Press, Cambridge, 1987).
- [8] D. Wu, C. Y. Zheng, C. T. Zhou, X. Q. Yan, M. Y. Yu, and X. T. He, *Phys. Plasmas* 20, 023102 (2013).
- [9] D. Wu, C. Y. Zheng, B. Qiao, C. T. Zhou, X. Q. Yan, M. Y. Yu, and X. T. He, *Phys. Rev. E* 90, 023101 (2014).
- [10] M. Tabak, J. Hammer, M. E. Glinsky, W. L. Kruer, S. C. Wilks, J. Woodworth, E. M. Campbell, M. D. Perry, and R. J. Mason, *Phys. Plasmas* 1, 1626 (1994).
- [11] D. Wu, C. Y. Zheng, and X. T. He, *Phys. Plasmas* 20, 063106 (2013).
- [12] Andreas J. Kemp, Robert E. W. Pfund, and Jurgen Meyer-ter-Vehn, *Phys. Plasmas* 11, 5648 (2004).
- [13] G. M. Petrov, J. Davis and Tz. Petrova, *Phys. Phys. Control. Fusion* 51 095005 (2009).
- [14] R. Mishra, P. Leblanc, Y. Sentoku, M. S. Wei, and F. N. Beg *Phys. Plasmas*, 20, 072704 (2013).
- [15] Yukap Hahn, *Physics Letter A* 23, 82, (1997).
- [16] Y. Hahn and J. Li, *Z. Phys. D* 36, 85 (1996).
- [17] P. Mansbach and J. Keck, *Phys. Rev.* 181, 275 (1969).
- [18] B. Makin and J. C. Keck, *Phys. Rev. Lett.* 11, 281 (1963).
- [19] G. Ecker and W. Kroll, *The Physics of Fluids* 6, 62, 1963.
- [20] John C. Stewart and Kedar D. Pyatt, JR. *Astr. Phys. Journal* 144, 1203, 1965.
- [21] O. Ciricosta, S. M. Vinko, H.-K. Chung, B. I. Cho, C. R. D. Brown, T. Burian, J. Chalupsky, K. Engelhorn, R. W. Falcone, C. Graves, V. Hajkova, A. Higginbotham, L. Juha, J. Krzywinski, H. J. Lee, M. Messerschmidt, C. D. Murphy, Y. Ping, D. S. Rackstraw, A. Scherz, W. Schlotter, S. Toleikis, J. J. Turner, L. Vysin, T. Wang, B. Wu, U. Zastra, D. Zhu, R. W. Lee, P. Heimann, B. Nagler, and J. S. Wark, *Phys. Rev. Lett.* 109, 065002 (2012).
- [22] M. Stransky, *Phys. Plasmas* 23, 012708 (2016).
- [23] Sang-Kil Son, Robert Thiele, Zoltan Jurek, Beata Ziaja, and Robin Santra, *Phys. Rev. X* 4, 031004 (2014).
- [24] Carlos A. Iglesias, Philip A. Sterne *High Energy Density Physics* 9, 103, (2013).
- [25] Thomas R. Preston, Sam M. Vinko, Orlando Ciricosta, Hyun-Kyung Chung, Richard W. Lee, Justin S. Wark, *High Energy Density Physics* 9, 258, (2013).
- [26] Wolfgang Lotz *Z. Physik* 232, 101 (1970).
- [27] Refer to "<http://physics.nist.gov/PhysRefData/ASD/>" for ionization energy data.
- [28] M. F. Gu, *Astr. Phys. J.* 582, 1241 (2003).
- [29] H. Xu, W. W. Chang, H. B. Zhuo, L. H. Cao, Z. W. Yue, *Chin. J. Comput. Phys.* 19, 305 (2002).
- [30] D. Wu, B. Qiao, C. McGuffey, X. T. He, and F. N. Beg *Phys. plasmas*, 21, 123118 (2014).
- [31] H. K. Chung, M. H. Chen, W. L. Morgan, Y. Ralchenko, R. W. Lee, *High Energy Density Physics* 1, 3, (2005).
- [32] Refer to "<https://www-amdis.iaea.org/FLYCHK/>" for online computing.